FLEXIBLE MICROINJECTOR FOR RAPID LOCALIZED DRUG DELIVERY FROM INGESTIBLE DEVICES

Joshua A. Levy[1,2,3], Michael A. Straker[2,3,4], and Reza Ghodssi[1,2,3,4,5]*
[1]Department of Materials Science and Engineering, [2]Institute for Systems Research,
[3]Robert E. Fischell Institute for Biomedical Devices, [4]Fischell Department of Bioengineering,
and [5]Department of Electrical and Computer Engineering
University of Maryland, College Park, USA

ABSTRACT

We present the first example of a microinjection device for rapid and localized drug delivery in the gastrointestinal (GI) tract. Oral drug delivery is overwhelmingly preferred by patients; however, drug efficacy is impaired by digestion and exclusion by the mucosal barrier. Although ingestible actuation technologies have shown potential for targeted treatment of GI tissues, drug administration is inefficient due to a reliance on passive diffusion in the turbulent GI environment. To address this, our flexible injector reassigns actuation force into pumping pressure to rapidly (<10 s) inject a 5.93 µL drug volume behind the mucosal barrier in the GI tract (Figure 1) using attainable actuation forces of 300 mN. This technology is enabled by an advanced hybrid 3D fabrication approach merging liquid-crystal display (LCD) vat photo-polymerization (VPP) 3D-printing of a compressible reservoir with direct laser writing (DLW) of sharp (~1 µm tip diameter) rigid microneedles. The flexible injector is a major step forward enabling more efficient and reliable localized oral drug delivery from ingestible devices.

KEYWORDS

Localized Drug Delivery, Microinjection, Ingestible Device, 3D Printing

INTRODUCTION

The gastrointestinal (GI) tract plays a key role in many bodily processes, and digestion of nutrients is the most prominent responsibility of this organ system.[1]-[3] Naturally, this makes the GI tract a desirable target for drug delivery as it acts as a gateway for selectively permitting entry of nutrients or drugs.[2] However, the selectivity of the intestinal tract, most significantly the mucosal barrier, poses significant challenges for oral delivery of drugs with certain charge and size.[4],[5] Among these drugs are many of the biological macromolecules used for highly effective modern therapies, including those for intestinal disease, cancer, and immunotherapies.[6] Moreover, the oral route to drug delivery is preferred by patients and results in better patient comfort and compliance.[7] Achieving drug injection in the GI tract would allow oral delivery of drugs that conventionally can only be delivered through parenteral routes.

Ingestible devices have shown the capacity to solve this problem by releasing drug into or around intestinal tissue for systemic or local treatment of disease, also enabling locational targeting to improve treatment efficacy while minimizing side effects.[8]-[12] Currently, the use of dissolving and passive diffusional systems for delivery results in drug loss to the lumen, and only diffusional transport in the tissue under the mucosal barrier.[13] Moreover, passive devices require attachment to the gastrointestinal wall for delivery due to the delivery timeframe.[14], [15] Previously, our group developed a diffusional injector that required anchoring barbs to attach to intestinal tissue.[16] Alternatively, bolus injection would enable rapid and forceful delivery of drugs to minimize device complexity and significantly improve transport toward vasculature and lymphatic capillaries for more efficient oral systemic therapy.

In this work, we have developed a hybrid-fabricated system that leverages a large, flexible reservoir with attached sharp and rigid microneedles to rapidly deliver drugs behind the mucosal barrier in the GI tract (Figure 1). The reservoir is fabricated by LCD-VPP 3D printing, and the microneedles are fabricated by a DLW process capable of ~1 µm feature resolution. In prior work, we have developed an actuator capsule that could compress this injector and rapidly inject drug into the intestinal tissue at locations of specific interest.[17] Modeling results showed the injector could be readily compressed with the given actuator force, and the excess force would supply sufficient pressure to quickly inject drug through the needle channels. Vacuum loading of the injector indicated a loading volume of 5.93 µL. The reservoir also showed the ability to use this actuator force to inject within 10 seconds and achieve enhanced convective flow when compared to a dissolving drug-loaded microneedle array, a commonly used approach in literature. Overall, this system enables reliable injection of drugs at local sites on command, making more effective treatment possible for a variety of disorders.

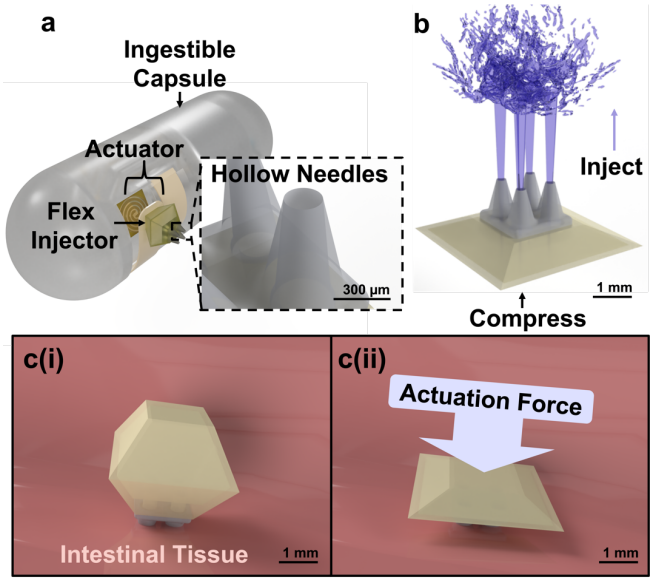

Figure 1. (a) Overview of actuator-enabled injection of drug from the flexible reservoir through the (b) hollow-channel microneedles. (c) Depiction of injection in the intestinal environment using an actuation force.

MATERIALS AND METHODS

The flexible injectors are fabricated by a hybrid approach combining LCD-VPP 3D printing and DLW to achieve meso-to-micro scale features effectively.

978-1-940470-05-4/HH2024/$25©2024TRF
DOI 10.31438/TRF.HH2024.18

Reservoir Fabrication

The flexible reservoir was designed in Autodesk Fusion 360® (San Francisco, CA, USA) to have a 25×25 mm base to insert into the direct laser writing (DLW) sample holder. Flexible reservoirs were designed with a pyramidal pedestal to attach to the base. The reservoirs have a height of 2.6 mm, a width of 3 mm, and a wall thickness of 150 µm. Stereolithography file types were exported and sliced in the CHITUBOX slicer program (Shenzen, CN) with a layer height of 50 µm and layer exposure time of 7 seconds. The flexible reservoir was fabricated by "liquid crystal display" (LCD) vat photo-polymerization (VPP) 3D-printing (Figure 2a-2b) using a Phrozen Sonic Mini 8K (Hsinchu City, Taiwan) with 3Dresyns (Barcelona, Catalonia, ES) Bioflex A50 MB biocompatible resin (A50 hardness; ISO 10993-5 compliant). Following printing, the part underwent ultrasonic cleaning in isopropanol for 5 minutes, repeating the process 3 times. The part was then cured in the Phrozen UV cure station for 45 minutes.

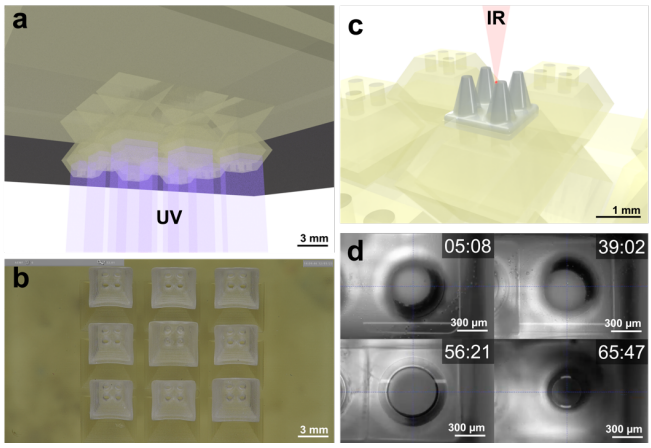

Figure 2. Fabrication of the microinjector with (a-b) LCD and (c-d) DLW process (50 µm interface overlap).

Microneedle Ex Situ Direct Laser Writing

Microneedles were printed directly on the reservoir surface using an ex-situ DLW process (esDLW) similar to that previously presented by Sarker *et al.* in 2023.[18] First, a biocompatible photoresin produced by Nanoscribe GmbH (Karlsruhe, DE), IP-Q, was vacuum loaded into the reservoirs. Microneedles, designed in Fusion 360®, have a 1.5×1.5 mm base with a 200 µm thickness. The four microneedles each have a 750 µm height with a 200 µm diameter injection channel and a 600 µm base diameter. Microneedle designs were sliced in the Nanoscribe DeScribe software with a 3 µm slicing distance, 50 mW laser power, and 100,000 µm/s scan speed. DLW of hollow microneedles was performed directly on top of the reservoir (Figure 2c-2d) using the Nanoscribe PPGT+ with the 10× objective. The reservoir/IP-Q interface was found manually, and the print was started 50 µm below the surface of the flexible reservoir to overlap the curing area and ensure proper interface adhesion between materials. Following printing the reservoir was submerged in Propylene Glycol Methyl Ether Acetate (PGMEA) to remove the remaining resin. To ensure removal of resin from the interior of the injector, the reservoirs were placed in a vacuum chamber and cycled between atmospheric pressure and vacuum.

Modeling of Injector Characteristics

Injector compression was evaluated using COMSOL Multiphysics 5.4 (Burlington, MA, USA) to understand the force required for compression. The Young's modulus of the Bioflex A50 resin was calculated to be 2.46 MPa as determined by the Shore A50 Hardness and established relationship between indentation hardness and modulus.[19] A range of forces were applied, and the compression response was evaluated (Figure 3a-3c). The flow rate through various channel sizes and applied pressures was assessed using the Hagen-Poiseuille equation (Figure 3d) in MathWorks MATLAB (Natick, MA, USA).

Microscopy of the Injector

The injector was imaged *via* LV-SEM (Figure 4) to visualize the injector structure and LCD-DLW interface. Injectors were attached to a sample stub and loaded into the Thermo Fisher Scientific XL SEM (Waltham, MA, USA) and imaged at 10 kV with a 60 Pa chamber pressure to minimize charging of the polymer surface.

Loading Volume Determination

Simulated drug, 0.1 %w/v FD&C Blue #1, was vacuum loaded into the injector using the three step process shown in Figure 5a. Samples were first submerged in the model drug solution then placed in a vacuum chamber. Air was evacuated from the chamber at a rate of ~0.05 Atm/min to minimize the potential for damage from pressure differences inside and out of the injector. Once reaching ~0.05 Atm, the injector was returned to atmospheric pressure at the same 0.05 Atm/min rate. During depressurization the air is pulled from inside the injector reservoir, then during pressurization the drug solution is forced to enter the reservoir. Following loading, the drug loading capacity was quantified by spectrophotometric evaluation (Figure 5c-5d). A calibration curve was previously determined for FD&C Blue #1 at the absorption wavelength of λ_{max}=629 nm. Loaded injectors were submerged in 10 mL of DI water and placed in an ultrasonic bath to prompt release of the dye into the surrounding liquid. The absorbance of the solution was determined using the Spectramax Plus 384 (San Jose, CA, USA) spectrophotometer to determine the final solution concentration. The reservoir volume was then determined using the final volume, final dye concentration, and initial dye concentration (n=6).

Simulated Drug Injection

Injection rate of the dye-loaded reservoir was visualized by emptying the injector into a water bath. A transparent cellulose acetate film was adhered to a 100 mm petri dish, and a ~1 mm diameter hole was formed as a support layer to allow force to be applied to the back of the injector. The petri dish was filled with water, acting as a medium to inject dye and evaluate flow after injection. The injector was filled with model drug, then the top of the injector was placed at the surface of the hole and a 300 mN force was applied to the back of the injector using a 30.5 g mass that was allowed to travel only in the vertical direction. The injection of dye was imaged from below and compared to a dissolving molded microneedle array of comparable volume (Figure 6a). Compression of the injector was also demonstrated in Figure 6b.

RESULTS AND DISCUSSION

Injectors were evaluated using a combination of modeling, microscopy, and benchtop characterization to ensure operability in the target environment.

Modeling of Injector Compression

It is critical to optimize the injector shape and thickness to ensure it can be readily compressed using the <500 mN force applied by the actuator,[17] while also maintaining a reasonable level of shape rigidity. Figure 3a-3c shows the deformation of the

microinjector under various compressive loads between 50 and 250 mN determined by COMSOL Multiphysics. The models revealed that the injector achieved full compression with a 300 mN force, allowing complete injection of fluid drug given the <500 mN criteria.

Forces higher than the required compression force will result in application of pressure on the fluid contained in the reservoir. This pressure will be responsible for pumping the fluid for injection. Modeling of channel flow (Figure 3d) using the Hagen-Poiseuille Equation was used to understand the rate of injection given a fixed pressure differential. Results indicated that a pressure of 200 Pa provided sufficient flow rate through the 200 µm needle channel, requiring only 0.5 mN excess force for rapid injection as calculated using the base surface area of the injector reservoir. Essentially, the excess pressure required for rapid injection of the ~6 µL volume is negligibly low; thus, rapid injection is readily achievable.

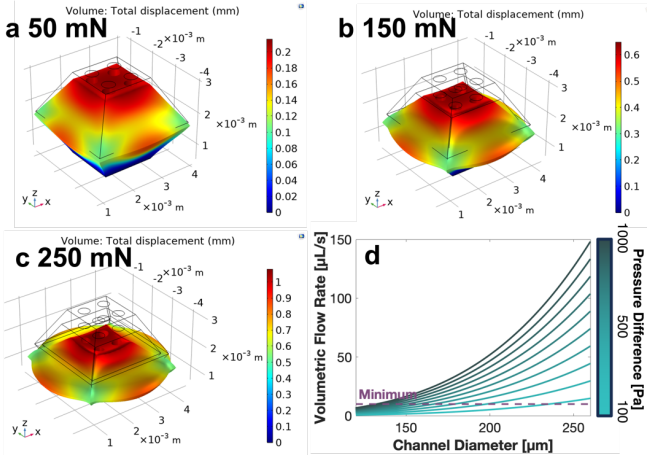

Figure 3. Modeling of the flexible injector rigidity and deformation response to applied forces of (a) 50 mN, (b) 150 mN, and (c) 250 mN. (d) Volumetric flow rate for 100-260 µm channels with a pressure difference of 100-1000 Pa. 200 Pa provides sufficient flow rate.

Injector Structure

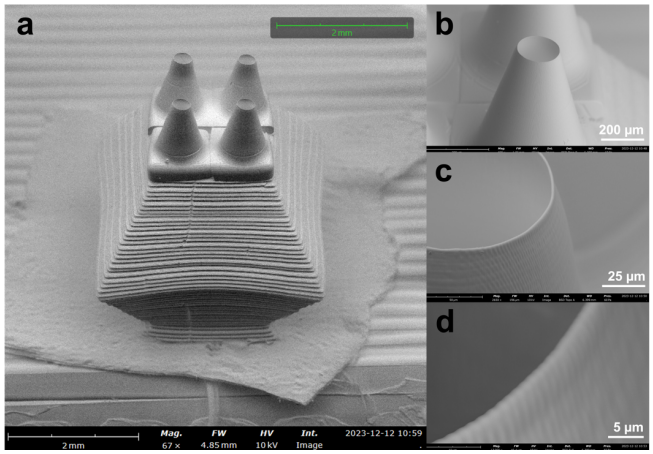

Figure 4. (a) SEM of the full injector showing the layered structure of the elastomeric flexible reservoir, needles and interface. (b) Top cone of the microneedle, and (c-d) magnified images of the sharp microneedle tip.

Microscopy of the injector revealed several key structural characteristics. Figure 4a shows the full injector, including the flexible reservoir and rigid microneedles. The flexible reservoir printed using LCD VPP 3D printing shows evidence of the layer-by-layer process as a stair-like surface on the injector walls. Moreover, the DLW process achieved a sharp ~1 µm tip diameter for facile tissue penetration (Figure 4b-4d). The hybrid process allows multi-scale fabrication, enabling relatively large features for large loading volumes, while also permitting high refinement and sharpness on the needles.

Vacuum Loading of Injectors

Injectors are vacuum loaded using the process shown in Figure 5a, where the injector is submerged, vacuum is drawn to remove air, and the chamber is repressurized to force entry of the drug liquid. Vacuum loading of injectors (Figure 5a) is theoretically capable of 97% loading efficiency limited by the vaporization pressure of water, 0.03 Atm at 25 °C (Figure 5b). However, repeated measurements determined a loading volume of 5.93±0.13 µL (n=6), 31.4% less than the theoretical loading volume. Deviation from the expected value in this case is expected to result from a combination of factors. Firstly, it is likely that surface tension around the channels of the injector could cause remnant bubbles around the entrance of the injector. More likely, geometric inaccuracies could result in reduced loading volume compared to the design volume. Commonly, photopolymer resins undergo shrinkage during curing, possibly resulting in a smaller overall reservoir volume. Moreover, residual compression of the injector could add to this error. In the future, the vacuum loading efficiency could be improved by using reservoir compression and vacuum to load the drug. Nevertheless, the scale of the injector could be readily adapted to carry far more drug.

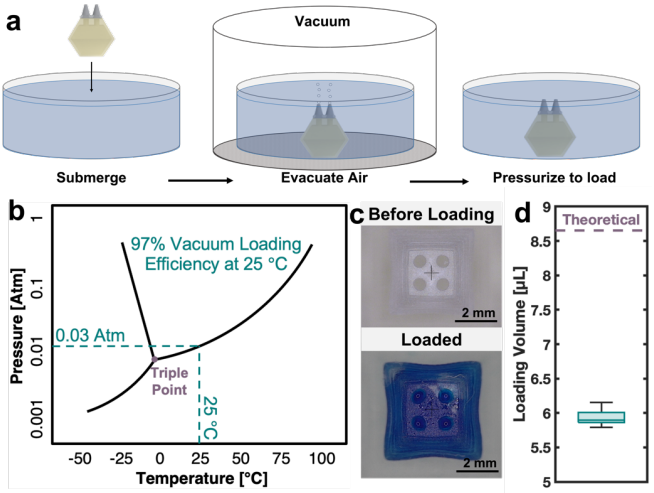

Figure 5. (a) Injector vacuum loading process and (b) corresponding generic phase diagram of water indicating up to 97% loading efficiency is possible. (c) Before and after dye loading. (d) Real and theoretical loading volume determined by spectrophotometry (n=6).

Simulated Drug Delivery

To evaluate the effect of convective delivery on transport after injection, flexible injectors were injected into a fluid bath and compared to standard molded microneedles. Figure 6 compares the rate of fluid delivery from the flexible injector module with standard dissolving molded microneedles. The flexible injector delivered the full dose in less than 10 s, while the dissolving microneedle took hours, showing over 100-fold improvement in delivery time compared to molded microneedles and the comparable standard drug tablets. Moreover, the demonstrated convective flow enhances

drug transport in the intestinal mucosa improving delivery efficiency. Overall, this flexible microinjector offers an integrative solution for rapid, localized submucosal oral drug delivery *via* ingestible capsules, potentiating enhanced care for patients suffering from both systemic and intestinal disease.

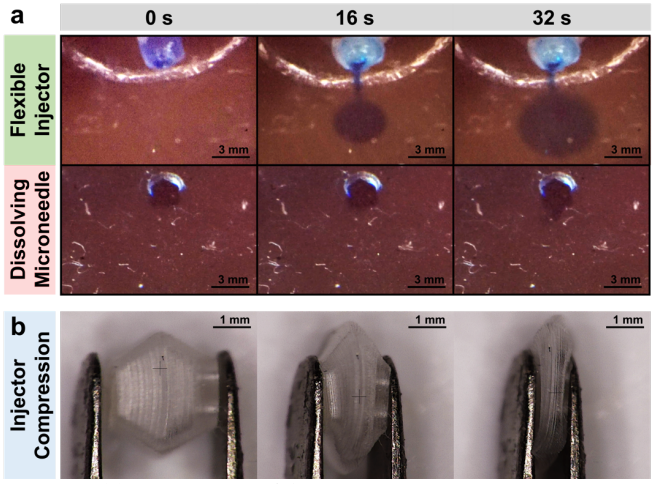

Figure 6. (a) Comparison of dye injection into water using injector and using dissolving microneedles at 0 s, 16 s, and 32 s showing significantly improved injection time and convective transport. (b) Flexible reservoir compression.

CONCLUSION

In this work, we demonstrate a flexible injection reservoir that can rapidly inject fluid drug into intestinal tissue by leveraging actuation force to create injection pressure. The injector, composed of a flexible reservoir fabricated by VPP 3D printing and sharp (~1 µm) rigid microneedles, held a volume of 5.93±0.13 µL. COMSOL FEM simulations and benchtop testing showed the ability to compress the injector and deliver drug in under 10 seconds. This new method of injection both reduces the practical burden of attaching to the GI wall for delivery and improves transport of drugs due to the convective flow. Overall, the flexible microinjector is a useful too that could be implemented in ingestible devices to improve the efficacy and tolerability of care for a myriad of diseases.

ACKNOWLEDGEMENTS

This work was supported by the national science foundation ECCS program under award #1939236. The authors acknowledge support from the Clark Doctoral Fellows Program, TerrapinWorks, the University of Maryland Nanocenter and its FABLAB.

REFERENCES

[1] J. N. Chu and G. Traverso, "Foundations of gastrointestinal-based drug delivery and future developments," *Nature Reviews Gastroenterology & Hepatology 2021 19:4*, vol. 19, no. 4, pp. 219–238, Nov. 2021, doi: 10.1038/s41575-021-00539-w.

[2] N. Volk and B. Lacy, "Anatomy and Physiology of the Small Bowel," *Gastrointest Endosc Clin N Am*, vol. 27, no. 1, pp. 1–13, Jan. 2017, doi: 10.1016/j.giec.2016.08.001.

[3] K. Geboes, K. P. Geboes, and G. Maleux, "Vascular anatomy of the gastrointestinal tract," 2001, doi: 10.1053/bega.2000.0152.

[4] H. C. Zierden *et al.*, "Avoiding a Sticky Situation: Bypassing the Mucus Barrier for Improved Local Drug Delivery," *Trends Mol Med*, vol. 27, no. 5, pp. 436–450, May 2021, doi: 10.1016/J.MOLMED.2020.12.001.

[5] S. P. Bandi, S. Bhatnagar, and V. V. K. Venuganti, "Advanced materials for drug delivery across mucosal barriers," *Acta Biomater*, vol. 119, pp. 13–29, Jan. 2021, doi: 10.1016/J.ACTBIO.2020.10.031.

[6] A. B. Pithadia and S. Jain, "Treatment of inflammatory bowel disease (IBD)," *Pharmacological Reports 2011 63:3*, vol. 63, no. 3, pp. 629–642, Dec. 2011, doi: 10.1016/S1734-1140(11)70575-8.

[7] M. S. Alqahtani, M. Kazi, M. A. Alsenaidy, and M. Z. Ahmad, "Advances in Oral Drug Delivery," *Front Pharmacol*, vol. 0, p. 62, Feb. 2021, doi: 10.3389/FPHAR.2021.618411.

[8] P. C. Valdivia, A. R. Robertson, N. K. H. De Boer, W. Marlicz, and A. Koulaouzidis, "An Overview of Robotic Capsules for Drug Delivery to the Gastrointestinal Tract," *Journal of Clinical Medicine 2021, Vol. 10, Page 5791*, vol. 10, no. 24, p. 5791, Dec. 2021, doi: 10.3390/JCM10245791.

[9] C. Steiger, A. Abramson, P. Nadeau, A. P. Chandrakasan, R. Langer, and G. Traverso, "Ingestible electronics for diagnostics and therapy," *Nat Rev Mater*, vol. 4, 2019, doi: 10.1038/s41578-018-0070-3.

[10] G. Traverso *et al.*, "Microneedles for Drug Delivery via the Gastrointestinal Tract," *J Pharm Sci*, vol. 104, no. 2, pp. 362–367, Feb. 2015, doi: 10.1002/JPS.24182.

[11] W. Chen *et al.*, "Dynamic omnidirectional adhesive microneedle system for oral macromolecular drug delivery," *Sci Adv*, vol. 8, no. 1, p. 1792, Jan. 2022, doi: 10.1126/SCIADV.ABK1792/SUPPL_FILE/SCIADV.ABK1792_MOVIES_S1_TO_S4.ZIP.

[12] H. Huang, Y. Lyu, and K. Nan, "Soft robot-enabled controlled release of oral drug formulations," *Soft Matter*, vol. 19, no. 7, pp. 1269–1281, Feb. 2023, doi: 10.1039/D2SM01624A.

[13] Z. Luo, N. Paunović, and J. C. Leroux, "Physical methods for enhancing drug absorption from the gastrointestinal tract," *Adv Drug Deliv Rev*, vol. 175, p. 113814, Aug. 2021, doi: 10.1016/J.ADDR.2021.05.024.

[14] J. A. Levy, M. A. Straker, J. M. Stine, L. A. Beardslee, V. Borbash, and R. Ghodssi, "Thermomechanical Soft Actuator for Targeted Delivery of Anchoring Drug Deposits to the GI Tract," *Adv Mater Technol*, vol. 8, no. 2, Jan. 2023, doi: 10.1002/ADMT.202201365.

[15] J. Lee, D. Kim, S. Bang, and S. Park, "Drug-Loaded Mucoadhesive Patch with Active Delivery and Controlled Releasing Ability," *Advanced Intelligent Systems*, vol. 4, no. 4, p. 2100203, Apr. 2022, doi: 10.1002/AISY.202100203.

[16] J. A. Levy, M. A. Straker, A. Colton, R. D. Sochol, and R. Ghodssi, "Anchoring Injector for Prolonged Delivery of Drugs in the Gastrointestinal Tract," in *Proceedings of the IEEE MEMS 2024 Conference*, 2024.

[17] J. A. Levy, M. A. Straker, L. A. Beardslee, and R. Ghodssi, "Cantilever Actuator Capsule for Magnetically Triggererd Drug Delivery in the GI Tract," in *IEEE Sensors*, Vienna, AT, Nov. 2023.

[18] S. Sarker *et al.*, "3D-Printed Microinjection Needle Arrays via a Hybrid DLP-Direct Laser Writing Strategy," *Adv Mater Technol*, vol. 8, no. 5, p. 2201641, Mar. 2023, doi: 10.1002/ADMT.202201641.

[19] A. N. Gent, "On the Relation between Indentation Hardness and Young's Modulus," *Rubber Chemistry and Technology*, vol. 31, no. 4, pp. 896–906, Sep. 1958, doi: 10.5254/1.3542351.

CONTACT

*R. Ghodssi, tel: +1-301-405-8158; ghodssi@umd.edu